



To study the Multimodality End-to-end Testing for Bilateral Metallic Implant in Pelvis

Pawan Kumar SINGH,¹ Deepak TRIPATHI,^{1,2} Rohit VERMA,¹ Sukhvair SINGH,³

Manindra BHUSHAN,⁴ Kothanda RAMAN,⁴ Soumitra BARIK,⁴ Gourav KUMAR,⁴

Munish GAIROLA⁴

¹Department of Physics, Amity Institute of Applied Sciences, Amity University, Noida (U.P.)-India

²Department of Physics, USAR, Guru Govind Singh University, Surajmal Vihar, New Delhi-India

³Radiological Physics & Internal Dosimetry Group, Institute of Nuclear Medicine & Allied Sciences, Defence Research & Development Organisation, New Delhi-India

⁴Division of Medical Physics, Department of Radiation Oncology, Rajiv Gandhi Cancer Institute and Research Centre, New Delhi-India

OBJECTIVE

The end-to-end (E2E) testing method enables understanding the difficulties and uncertainties in treating any specific case type. This study was focused on bilateral metallic implant cases.

METHODS

The study was performed on a cylindrical phantom of Perspex with holes for implant inserts. Two stainless steel metal rods of 7.5–8.0 g/cc mass density were inserted in the phantom. The ionization chamber CC13 was kept at a 5 cm depth in the phantom. The phantom was scanned on a computed tomography simulator in pelvis protocol with a 1mm slice thickness. The scans were imported to the contouring station without applying artifacts correction. Chamber volume was contoured as gross tumor volume (GTV); margin to GTV, clinical target volume, and planning target volume were created. Four isocentric plans (Conventional, three-dimensional conformal radiotherapy[3D-CRT], intensity-modulated radiotherapy [IMRT], and volumetric-modulated radiotherapy [VMAT]) were generated for two Linacs-Truebeam (TB)-sTx and 2300-CD. The conventional plan was a single anterior field, 3D-CRT was four field box techniques, IMRT was seven field plan, and VMAT was with two complete arc. Pre-treatment verification was done using CBCT. Four plans were created on helical tomotherapy with different prescriptions and delivered using MVCT guidance.

RESULTS

In conventional plans, variations were –1.40%, –1.57%, and for 3DCRT, variations were –5.08% and –4.93%, for IMRT, the differences between measured and TPS doses were 1.84 % and –1.55% for VMAT plans, and the variations were 0.68% and –0.88% for TB and 2300-CD, respectively. The tomotherapy plans with gradient showed deviations more significant than 3%. Similarly, the variations for single prescription plans were within 3%.

CONCLUSION

The phantom design used in the test provided a comprehensive understanding of simulation and delivery problems.

Keywords: End-to-end; metallic implant; MVCT; phantom study.

Copyright © 2023, Turkish Society for Radiation Oncology

Received: December 09, 2022

Revised: February 14, 2023

Accepted: April 11, 2023

Online: May 03, 2023

Accessible online at:

www.onkder.org

OPEN ACCESS This work is licensed under a Creative Commons Attribution-NonCommercial 4.0 International License.



Dr. Pawan Kumar SINGH

Department of Physics,

Amity Institute of Applied Sciences,

Amity University, Noida (U.P.)-India

E-mail: pawansingh786125@gmail.com

INTRODUCTION

Multiple physical ailments and cancer, an old-age disease, have been caused by changing lifestyles, eating habits, and work cultures.[1] After the age of 40, people tend to have bone weakness, slipped disks, and osteoporosis. These patients may require surgical interventions to stabilize their bone fractures, misalignments, and prosthetic implants.[2] Osteoarthritis damages the hip joints, and the patient needs artificial joints. Different metallic alloys are used to make artificial implants.[3] Globocan-2020 data indicate that in this population, 10.7% of Colorectum and 7.3% of prostate cancer cases are added annually.[4] The probability of patients with metallic implants undergoing cancer treatment is high. Stereotactic body radiation (SBRT) in prostate cancer and short-course radiotherapy in colorectum is the standard of care for these sites.[5]

Intensity-modulated radiotherapy (IMRT) and volumetric-modulated radiotherapy (VMAT) are advanced treatment techniques that involve multiple levels of computer and manual interferences to execute the treatment delivery.[6] Patient-specific quality assurance (QA) is integral to high-end treatment modalities. The patient-specific QA is performed using point dose measurements, fluence measurements, and computer algorithms.[7,8] The point dose and fluence measurements are carried out on homogeneous phantoms, which do not account for any heterogeneity inside the patient.

Patients having metallic implants pose multiple problems during radiotherapy treatment. The streak artifacts in simulation images cause difficulty in identifying the organ borders, leading to inaccurate target and organ-at-risk delineation during contouring.[9] The dose calculation algorithms do not account for any artifacts in computed tomography (CT) images, causing wrong dose calculation.[10,11] The treatment delivery also requires multiple imaging for treatment setup verification; the artifacts also create issues while verifying the setup.[12]

The end-to-end (E2E) test includes all the steps in patient treatment. It starts with positioning, imaging, contouring, and treatment planning and ends with setup verification and delivery. The test includes all the systematic and random errors in the treatment procedure and is one of the best ways to check the overall uncertainty.[13] Brodbek et al.[14] performed an E2E test using Ruby phantom and validated multiple target treatments by point dose measurements. Furuya et al.[15] did a multi-institutional E2E test study for spine SBRT. They concluded that the treat-

ment dose could be calculated within $\pm 5\%$ despite the metal inserts inside the phantom. Zakjevskii et al.[16] developed a head and neck phantom to validate the IMRT treatment. These studies motivated us to conduct an E2E test on hip prosthesis cases.

In this study, we used an in-house phantom having provisions for the implant. The phantom was designed to study the E2E treatment delivery issues in bilateral hip implant patients. The study used three different treatment delivery machines (Truebeam [TB], Clinac ix, and helical tomotherapy [HT]) from two vendors to avoid and understand the problems associated with the other vendors and within the same vendor.

MATERIALS AND METHODS

Phantom Design

A phantom was designed to simulate the human pelvis geometry with different insert options, as shown in Figure 1a. It was cylindrical with a length of 21 cm and a diameter of 20 cm and made up of polymethyl methacrylate. A hemispherical head of diameter 20 cm was also attached to the phantom's superior part. To simulate the femur implants, two stainless steel rods, right (length = 22.7cm, diameter = 2.1 cm) and left (length = 20.9cm, diameter = 2.1 cm) of 7.5–8g/cc mass density, were inserted into the phantom.

Dosimetry System

The point dose verification method was used to perform the dosimetric verification. The CC13 ionization chamber (0.13 cc) (IBA Dosimetry, Germany) was kept at a 5 cm depth from the anterior surface of the phantom. The lateral distance from both implants was 5cm.

Simulation and Contouring

The phantom was positioned on the CT scanner couch and aligned with the help of lasers for proper setup. The setup position was marked with radio-opaque markers. The CT scan was performed on Somatom Sensation open (Siemens Healthneers, Germany) and was reconstructed in 1 mm slice thickness. The planning scans were exported to the contouring stations Eclipse (Version: 15.5, Varian Medical Systems, Palo Alto, CA). The different target volumes were delineated to simulate the anatomy and treatment geometry. The chamber volume was contoured and was termed as gross tumor volume (GTV); a clinical target volume (CTV) was created with 5mm uniform margin around the GTV, and a further 7mm uniform margin to it was the planning target volume (PTV). The metallic rods were con-

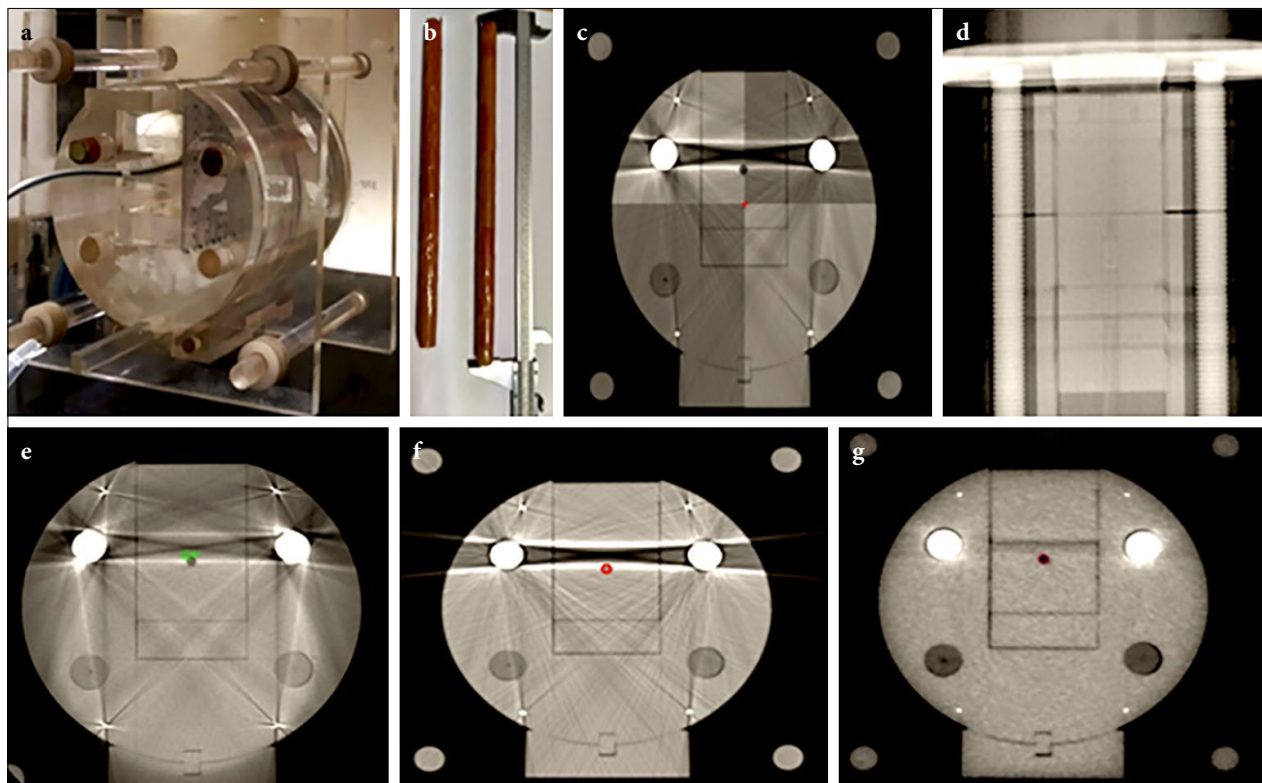


Fig. 1. (a) The phantom image, (b) the implanted rods, (c) the CBCT and CT image Matching axial view, (d) the 2D-MV image of the phantom, (e) the CBCT image axial view, (f) the CT image axial view, and (g) the MVCT image. CBCT: Cone-beam CT; CT: Computed tomography; 2D-MV: Two dimensional Mega voltage; MVCT: Mega-voltage CT.

toured and named RT implant and Lt Implant. Streak artifacts were contoured in a structure called an “artifact.” These contours were used in the planning optimization and evaluated for dosimetry.

Treatment Planning

Two different planning systems were used to create the treatment plans: Eclipse treatment planning stations for Varian machines (Version:15.1, Varian Medical Systems, Palo Alto, CA) and Accuray Precision software for HT(Accuray Precision 2.0.1.1,[5] Accuray Inc. Sunnyvale, CA).

Planning on Varian Machines

TBsTx (Varian Medical Systems, Palo Alto, CA) was an advanced linear accelerator capable of delivering conventional, three-dimensional conformal radiotherapy (3D-CRT), IMRT, and VMAT treatment techniques. The machine was equipped with high-definition multi-leaf collimators (HD-MLCs), having a maximum travelling speed of 2.5 cm/s. It had a collimator Jaw tracking system and operated on a digital platform. HD-MLCs consists of 60 pairs of MLCs leaves; 32 pairs in the center had an isocenter projection of 2.5 mm, and 14 pairs on

either side which had an isocenter projection of 5 mm. The second machine was the Clinac-ix series, 2300-CD, also known as the rapid arc(RA) from Varian (Varian Medical Systems, Palo Alto, CA), which could also deliver advanced treatments similar to TB. This machine had millennium multi-leaf collimators(MLCs),which consists of 60 pairs of MLCs leaves; 40 pairs in the center had an isocenter projection of 5mm, and ten pairs on either side had an isocenter projection of 10mm. The leaves travel at the same speed as HD-MLCs and was operated on an analog platform without jaw tracking. Each plan was created separately for both machines. The plans were calculated using a 2.5 mm grid size and analytic anisotropic algorithm version(15.6.06).

Conventional Treatment Plans

The conventional treatment plans were created using the 6MV photons, 10×10 cm² field width with gantry, collimator, and couch angles set to be zero. The monitor unit (MU)-based calculation method was used, and 300 MUs were used to calculate the plan. The beam did not face any implant in its path but passed through the streak artifact created by the implant to deliver the dose

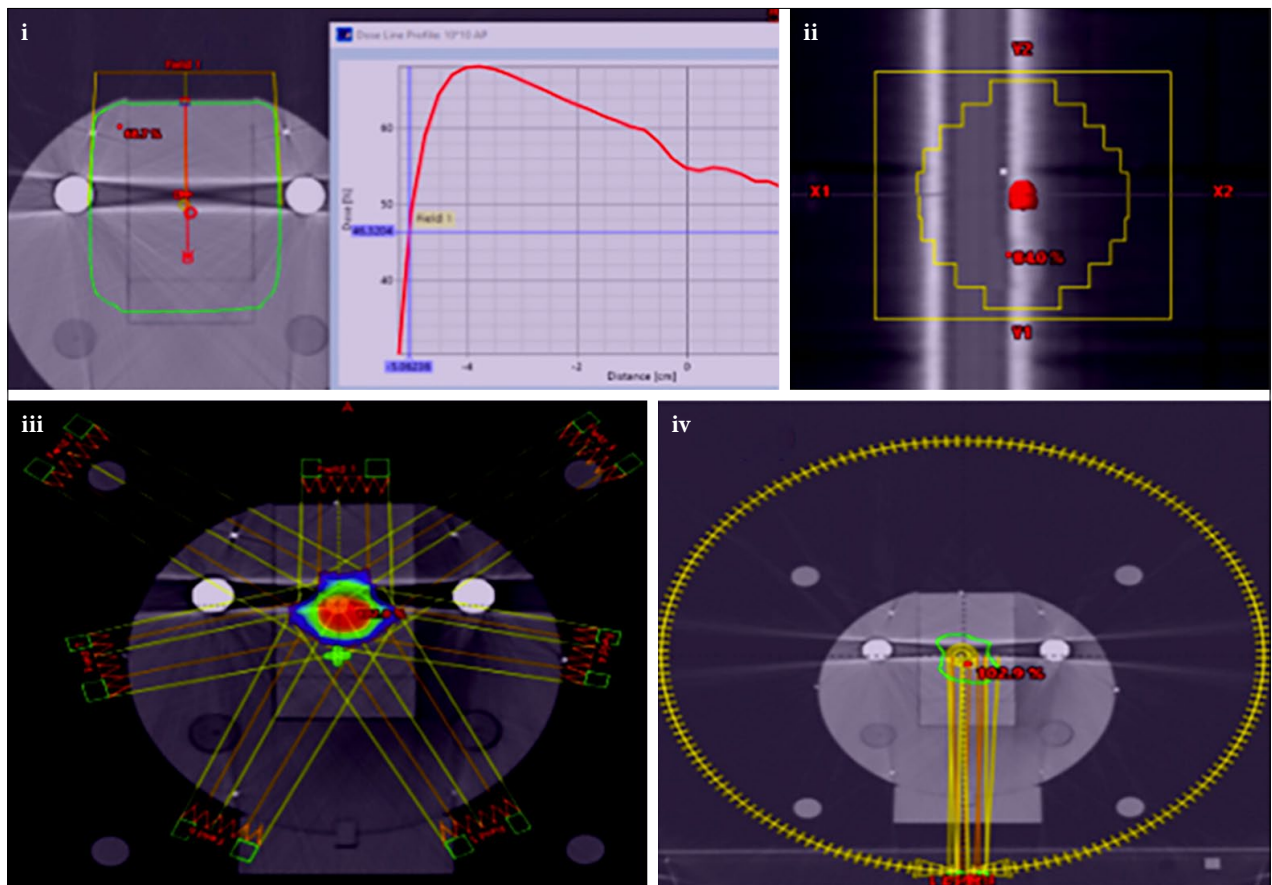


Fig. 2. (i) The Conventional plan on TB, the graph tagged to it shows the dose profile perturbation due to artifact, (ii) in 3D-CRT, the beams eye view showed the partial occlusion of the target by implant material, (iii) IMRT plan beam arrangement avoiding implant, (iv) the VMAT plan beam geometry.

TB: Truebeam; 3D-CRT: Three-dimensional conformal radiotherapy; IMRT: Intensity-modulated radiotherapy; VMAT: Volumetric-modulated radiotherapy.

to the target Figure 2 (i). TB and 2300CD plans were named TB1 and RA1, respectively.

3D-CRT Treatment Planning

3D-CRT plans were four-field box technique plans with 6MV, in which gantry angles were 0° , 180° , 90° , and 270° without couch and collimation angle. The MLCs were used to conform the PTV, and a 7mm margin was given to compensate for the penumbra and setup errors. In this plan, the implant material partially obstructed the lateral beams (90° and 270°). The MU-based calculation method was used, and 154 MUs were used in each field to calculate the plan. TB plan was called TB2, and 2300CD plans were named as RA2.

IMRT Planning

The IMRT plans were seven-beam co-planar IMRT plans with gantry angles of 0° , 51° , 102° , 153° , 204° , 255° , and 306° without collimation. The beams were placed

in such a way that the beam's entry should not face the implanted material. The plans were optimized using a photon optimizer (PO) (version:15.6.06) for 5Gy per fraction dose to CTV. TB plans were named TB3, and 2300CD plans were termed RA3. Figure 2. (iii) shows the beam arrangement of IMRT plans avoiding the implants.

VMAT Planning

VMAT provides the optimizer with higher degrees of freedom to achieve the target and organ objectives. MLC, gantry, and dose rate modulation in the treatment beam lead to a highly conformal VMAT plan. [17] VMAT plan with two complete arcs: clockwise (181° - 179°) and anti-clockwise (179° - 181°) without any collimation and couch were optimized using PO for 5Gy per fraction dose to CTV. The optimizer used an inbuilt option(exit-only) to avoid the beam's entry through the implant. TB plans were named TB4, and 2300CD plans were called RA4.

HT Plans

The plans were created for the Radixact X9 treatment delivery system (Radixact X9, Accuray Inc. Sunnyvale, CA). The machine was equipped with 6 MV flattening filter-free photon beams for treatment delivery, and it could deliver helical IMRT and tomo-direct (3D-CRT) plans. It had dynamic and fixed jaw treatment delivery options. Three jaw settings were $40 \times 1 \text{ cm}^2$, $40 \times 2.5 \text{ cm}^2$, and $40 \times 5 \text{ cm}^2$; dynamic jaw options were available with the latter two settings. It had the binary MLC leaves consisting of 64 leaves, each having projection of 6.25 mm at the isocenter. The helical treatment delivery was the mode in which the couch moved constantly, and the ring gantry moved continuously and delivered a modulated fan beam. A mega-voltage CT (MVCT) of 3.2 MV was onboard, and available for image guidance on tomotherapy. The structures delineated on the eclipse contouring station were transferred to the Accuray Precision planning. All HT plans were created such that the entry of the beams does not face the implant material directly into its path using the planning optimizer. The HT plans were calculated using the convolution superposition algorithm.

Plans without Overwritten Density

Plan HT1 was helical delivery mode, IMRT, with dynamic jaws (field width $40 \times 5 \text{ cm}^2$), pitch 0.172, and modulation factor 2. The plan GTV was optimized for 5 Gy, and PTV was for 2 Gy per fraction. Plan HT3 was IMRT with dynamic jaws (width $40 \times 2.5 \text{ cm}^2$), pitch 0.172, and modulation factor 1.5. This plan was optimized to deliver 5Gy for a single target CTV, calculated, and approved for the treatment delivery.

Plans with Overwritten Density

A CT scan region without artifacts was used to obtain the density for overwriting the artifact region. Plan HT2 was created using similar settings as HT1, except the "artifact" was overwritten with a mass density of 1.087 g/cc. The plan was optimized and calculated with this overwritten density and approved for treatment. The plan HT4 was again optimized with the equal objectives and settings as HT3. In this plan, the structure "artifact" densities were overwritten. The plan was approved for treatment delivery.

Treatment Delivery Systems

For TB, we aligned the phantom using the external markers placed over it and with the help of room lasers. We applied the shifts according to the plan isocenter. Mega-voltage (MV) images were acquired from an electronic portal imaging device, and an onboard imager did kilo-voltage (KV) imaging; MV-KV pair 2D

images were gathered to verify the phantom alignment. The cone-beam CT (CBCT) (Onboard Imager 1.6, Varian Medical Systems, Inc. Palo Alto, CA) was performed using the pelvis scanning protocol. The chamber volume and implanted materials were matched in 3D-matching and applied the shifts obtained. The treatment plan was delivered on the phantom, and doses were measured in the ionization chamber contoured as GTV. All the plans had the same setup isocenter, so only the 3D matching was done after plan TB1. We repeated this process on Clinac-ix 2300 CD (RA) for setup verification and treatment delivery.

The phantom was aligned with red lasers for Radixact X9 tomotherapy, and an MVCT scan was taken to confirm the phantom location. The GTV and implants were matched, and the treatment was executed after applying the shifts.

Dose Measurement and Analysis

The CC13 ionization chamber (Model CC13, IBA Dosimetry GmbH, Schwarzenbruck, Germany) (volume: 0.13 cc), in combination with the Wellhofer Dose1 electrometer, was used for the point dose measurements. All the correction factors, the temperature and pressure (Ktp) and dose to water (Ndw), were used to calculate the dose. The mean doses from the treatment planning system (TPS) and the doses measured in the ion chamber were used to calculate the % variation. The formula used was:

$$\% \text{Difference} = \frac{\text{Measureddose} - \text{TPSdose}}{\text{Measureddose}} \times 100$$

RESULTS

Setup Verification

In all the machines, we exposed the phantom with image guidance; Figure 1d shows the initial setup MV image; Figure 1c shows the 3D matching with the acquired CBCT. The shifts were less than 1mm before the execution of the plan. Figure 1g was MVCT acquired with the tomotherapy; the shifts were <1 mm for HT plans.

Dosimetric Measurements

Table 1 shows the detailed comparison between measured and TPS calculated doses. In the conventional plans TB1 and RA1, the dose variations were -1.40% and -1.57%, respectively. The plans TB2 and RA2, the variations were -5.08%, and -4.93%, respectively. For IMRT plans TB3 and RA3, the differences between measured and TPS doses were 1.84 % and -1.55%, respectively. Similarly, for VMAT plans TB4 and RA4, the variations were 0.68% and -0.88%.

Table 1 Point dose measurements

Plan name	Measured dose (cGy)	TPS dose (cGy)	% DIFF
RA1	262	266.12	-1.57
RA2	386.32	405.38	-4.93
RA3	498.12	505.86	-1.55
RA4	495.84	500.18	-0.88
TB1	265.47	269.18	-1.40
TB2	386.44	406.08	-5.08
TB3	509.26	499.9	1.84
TB4	514.4	510.9	0.68
HT1	492.79	509.2	-3.33
HT2	491.07	508.4	-3.53
HT3	490.21	501.6	-2.32
HT4	489.92	501	-2.26

TPS: Treatment planning system; DIFF: Difference between measured and TPS dose; RA: Rapid Arc (2300-CD); TB: Truebeam; HT: Helical tomotherapy; Gy: Gray

The tomotherapy plans with gradient HT1 and HT2 showed more significant deviations HT1 (-3.33%) and HT2 (-3.53 %). Similarly, the variations for single prescription plans were within 3% HT3 (-2.32%) and HT4 (-2.26%).

DISCUSSION

The phantom-based E2E test showed the reproducibility of the setup and the geometric information for all three machines. The phantom 3D-image showed that the artifacts created near the target almost blurred everything; the streak artifacts showed air-like patches near the target. These artifacts created may blur the walls of the bladder and rectum in prostate cases and may mislead in making decisions for advanced SBRT treatment modality.[18] The 2D-image verification provided a clear orientation of phantom alignment with metallic implants; the artifacts were minimal in these images. The AAPM TG-63[19] also recommended verifying the lateral beam's eye view using the portal imaging device. The 3D images pose challenges for organ matching. The multiple projections used in reconstructing the 3D images have perturbed photon profiles due to the scattered data leading to the artifacts. The CBCT uses KV beams, and the low-energy photons scattering is more compared to the high-energy photons.[20] In addition, the MVCT images had fewer artifacts than their counterparts in the presence of metallic objects. Therefore, the MVCT showed better 3D-matching compared to the CBCT. Aubin et al.[21] compared the CBCT and MVCT images and suggested that the missing tissue contours can be delineated

with the help of MVCT images. Sterzing F et al.[22] conducted a study on MVCT images for treatment planning. They concluded that the images had limitations due to a reduced soft-tissue contrast but consistently demonstrated advantages in patients with metal implants. These observations suggest that the MVCT images were superior to the KV-CBCT images for the metallic implant cases. Chapman et al.[23] concluded that the MVCT images show better visualization of the organ at risk and target in their study of planning bilateral hip prostheses. However, the imaging doses will be a matter of concern for the MVCT setup verification protocols. These publications studied the imaging device and the doses associated with them for radiation therapy.[24–26] They concluded that the imaging doses depended on the scan length and energy used. Therefore, the MVCT regime can be practiced for shorter treatment schedules, where the imaging doses will be less during treatment, and artifacts will be dealt with better precision.

Analysis of different techniques showed that in the conventional plans where the beam did not face any implant found, the dosimetric variations of <2%, that is, within the tolerance of $\pm 3\%$.[27] The results indicated that the artifact did not impact the dose calculation and delivery in single anterior fields. In Figure 2 (i), the axial cut of the CT slice and the graph tagged to it showed the streak artifacts in the beam paths and the variation in percentage dose from the surface to the target; at the location of the streak artifact, observed a dip in percentage depth dose. There were higher deviations in 3D-CRT plans when the treatment beams were partially occluded from the lateral sides of 90° and 270° gantry angles.[28] Figure 2 (ii) shows the beam's eye view of one of the lateral beams. The outcome suggested that the 3D-CRT treatment planning should be carried out using beam eye-view, avoiding the beams facing the implant directly.[19] Mahuvava et al.[29] conducted a monte carlo study with a similar beam arrangement, and their results also showed dose loss in the lateral beams. The variations for IMRT plans TB3 and RA3 were less than $\pm 2\%$. Therefore, the results suggest that the beam arrangement for IMRT Figure 2 (iii) avoiding the implants works properly. Kung et al.[30] conducted an IMRT planning strategy using nine fields avoiding the implants and found similar results. Similarly, the VMAT plans' variations were less than $\pm 1\%$. Therefore, the software optimization options avoided the implant correctly.[31,32] The variations shown in Table 1 suggest that the machine-to-machine variation among the same vendor is negligible; only the effect of planning techniques was significant for Varian machines.

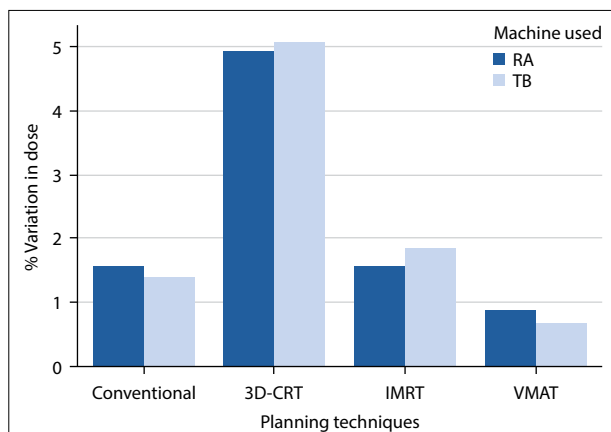


Fig. 3. Variation of doses in Varian machines for different techniques.

RA: Rapid Arc (2300 -CD); TB: Truebeam; 3D-CRT: Three-dimensional conformal radiotherapy; IMRT: Intensity-modulated radiotherapy; VMAT: Volumetric-modulated radiotherapy.

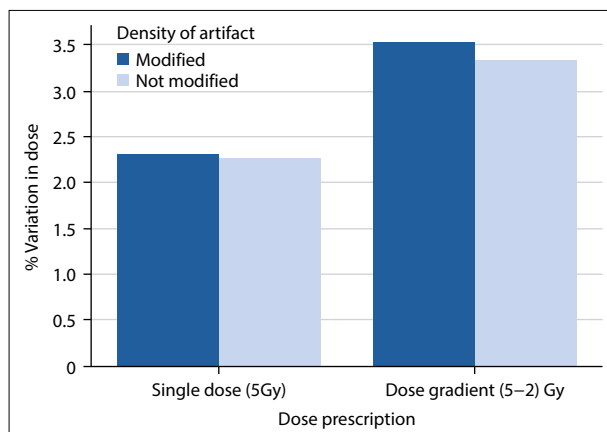


Fig. 4. Variation of doses in tomotherapy plans for different dose prescriptions.

Gy: Gray.

This was indicated in the bar graph. Figure 3 shows the compatibility of two machines for the same case using different techniques. The inter-technique differences were significant than the inter-machine variation.

The set of tomotherapy plans HT1 and HT2 had variations of more than the $\pm 3\%$; the probable cause would be the gradient created just beyond the target, that is, chamber volume.[27] Density overwrites had a negligible impact on the treatment strategy. Likewise, there were less than 3% variations in the plans when we optimized them for a uniform prescription. In these plans also, the effect of density overwrite was minimal. Figure 4 shows the compatibility of the plans having the same dose objectives; the density overwrites had minimal effect on the treatment delivery of the plans. Further, it indicates that the plans with the dose gradient need proper attention during implementation to avoid higher dose variations in planned and delivered doses.

Gallo et al. conducted a similar study for spine cases and found that the machines could deliver equivalent results.[33] Le et al.[34] studied uncertainties in dose for hip implant patients using human cadavers and alkaline dosimeters. They reported up to 20% variations for the different regions near the implant. In this study, Table 1 observations indicated the maximum variation of 5%; but it only includes the variation in the target dose; the dosimetric variations near the implant need to be studied.

This study observed all the variations and implementation-related issues with prosthesis patients. Results can be used in decision-making, setting up the departmental protocols for implant patients and further can be used for intercomparison. The absence of actual

bladder and rectum densities was the limitation of this study. Future research must consider non-coplanar beams and metal reduction algorithms.[35]

CONCLUSION

The phantom design used in the E2E test provided a comprehensive understanding of simulation and delivery problems. IMRT and VMAT techniques using beam avoidance were the best approach for planning on Varian machines. In tomotherapy, MVCT images were adequate for visualizing treatment geometry. The plan implementation in the gradient regions must be verified to avoid delivery errors. The variations in delivery techniques for the two vendors helped us decide the departmental protocol for the prosthesis cases.

Acknowledgments: The authors thank the management of Rajiv Gandhi Cancer Institute and Research Centre in New Delhi, India, for their continued support and encouragement to complete this research. We also thank Dr. Lalit Kumar for his guidance and support in the research process.

Peer-review: Externally peer-reviewed.

Conflict of Interest: All authors declared no conflict of interest.

Financial Support: None declared.

Authorship contributions: Concept – P.K.S., D.T., R.V.; Design – S.S., P.K.S., R.V., M.B.; Supervision – P.K.S., R.V., D.T., S.S., M.B., M.G., G.K.; Materials – P.K.S., M.G., M.B., G.K., S.B., K.R.; Data collection and/or processing – P.K.S., G.K., M.B., S.B., K.R., M.G., S.S.; Data analysis and/or interpretation – P.K.S., M.B., G.K., S.S., R.V., D.T., S.B., K.R., M.G.; Literature search – P.K.S., M.G., M.B., K.R., S.B., D.T., R.V.; Writing – P.K.S., R.V., S.S., D.T., S.B.; Critical review – M.G., M.B., K.R., S.S., D.T., R.V.

REFERENCES

1. Laconi E, Marongiu F, DeGregori J. Cancer as a disease of old age: changing mutational and microenvironmental landscapes. *Br J Cancer* 2020;122:943–52.
2. Davis R, Singh A, Jackson MJ, Coelho RT, Prakash D, Charalambous CP, et al. A comprehensive review on metallic implant biomaterials and their subtractive manufacturing. *Int J Adv Manuf Technol* 2022;120(3-4):1473–530.
3. Merola M, Affatato S. materials for hip prostheses: a review of wear and loading considerations. *Materials* 2019;12(3):495.
4. IARC. Global Cancer Observatory. Available at: <https://gco.iarc.fr/>. Accessed Jan 12, 2022.
5. Cihan Y. The role and importance of SBRT in prostate cancer. *Int Braz J Urol* 2018;44(6):1272–4
6. Teoh M, Clark CH, Wood K, Whitaker S, Nisbet A. Volumetric modulated arc therapy: a review of current literature and clinical use in practice. *Br J Radiol* 2011;84(1007):967–96
7. Xia Y, Adamson J, Zlateva Y, Giles W. Application of TG-218 action limits to SRS and SBRT pre-treatment patient specific QA. *J Radiosurg SBRT* 2020;7(2):135–47.
8. Stern RL, Heaton R, Fraser MW, Goddu SM, Kirby TH, Lam KL, et al; AAPM Task Group 114. Verification of monitor unit calculations for non-IMRT clinical radiotherapy: report of AAPM Task Group 114. *Med Phys* 2011;38(1):504–30.
9. Roth TD, Maertz NA, Parr JA, Buckwalter KA, Choplin RH. CT of the hip prosthesis: appearance of components, fixation, and complications. *Radiographics* 2012;32(4):1089–107.
10. Das IJ, Kahn FM. Backscatter dose perturbation at high atomic number interfaces in megavoltage photon beams. *Med Phys* 1989;16(3):367–75.
11. AAPM Radiation Therapy Committee, Task Group No. 65 and American Association of Physicists in Medicine. Tissue inhomogeneity corrections for megalovoltage photon beams, report no. 085. Available at: <https://www.aapm.org/pubs/reports/detail.asp?docid=86>. Accessed Apr 24, 2023.
12. Kaur I, Rawat S, Ahlawat P, Kakria A, Gupta G, Saxena U, et al. Dosimetric impact of setup errors in head and neck cancer patients treated by image-guided radiotherapy. *J Med Phys* 2016;41(2):144–8.
13. Schmidhalter D, Malthaner M, Born EJ, Pica A, Schmuecking M, Aebersold DM, et al. Assessment of patient setup errors in IGRT in combination with a six degrees of freedom couch. *Z Med Phys* 2014;24(2):112–22.
14. Brodbek L, Kretschmer J, Büsing K, Looe HK, Poppe B, Poppinga D. Systematic end-to-end testing of multiple target treatments using the modular RUBY phantom. *Biomed Phys Eng Express* 2021;8(1).
15. Furuya T, Lee YK, Archibald-Heeren BR, Byrne M, Bosco B, Phua JH, et al. Evaluation of multi-institutional end-to-end testing for post-operative spine stereotactic body radiation therapy. *Phys Imaging Radiat Oncol* 2020;16:61–8.
16. Zakjevskii VV, Knill CS, Rakowski JT, Snyder MG. Development and evaluation of an end-to-end test for head and neck IMRT with a novel multiple-dosimetric modality phantom. *J Appl Clin Med Phys* 2016;17(2):497–510.
17. Kumar L, Yadav G, Raman K, Bhushan M, Pal M. The dosimetric impact of different photon beam energy on RapidArc radiotherapy planning for cervix carcinoma. *J Med Phys* 2015;40(4):207–13.
18. Fischer AM, Hoskin PJ. Radiotherapy-induced toxicity in prostate cancer patients with hip prostheses. *Radiat Oncol* 2022;17(1):9.
19. Reft C, Alecu R, Das IJ, Gerbi BJ, Keall P, Lief E, et al; AAPM Radiation Therapy Committee Task Group 63. Dosimetric considerations for patients with HIP prostheses undergoing pelvic irradiation. Report of the AAPM Radiation Therapy Committee Task Group 63. *Med Phys* 2003;30(6):1162–82.
20. Wellenberg RH, Boomsma ME, van Osch JA, Vlassenbroek A, Milles J, Edens MA, et al. Low-dose CT imaging of a total hip arthroplasty phantom using model-based iterative reconstruction and orthopedic metal artifact reduction. *Skeletal Radiol* 2017;46(5):623–32.
21. Aubin M, Morin O, Chen J, Gillis A, Pickett B, Aubry JF, et al. The use of megavoltage cone-beam CT to complement CT for target definition in pelvic radiotherapy in the presence of hip replacement. *Br J Radiol* 2006;79(947):918–21.
22. Sterzing F, Kalz J, Sroka-Perez G, Schubert K, Bischof M, Roder F, et al. Megavoltage CT in helical tomotherapy - clinical advantages and limitations of special physical characteristics. *Technol Cancer Res Treat* 2009;8(5):343–52.
23. Chapman D, Smith S, Barnett R, Bauman G, Yartsev S. Optimization of tomotherapy treatment planning for patients with bilateral hip prostheses. *Radiat Oncol* 2014;9:43.
24. Karaca S, Başaran H. Megavoltage computed tomography (MVCT) dose assessment at different depths. *RAD Conference Proceedings* 2018;3:169–73.
25. Ding GX, Alaei P, Curran B, Flynn R, Gossman M, Mackie TR, et al. Image guidance doses delivered during radiotherapy: Quantification, management, and reduction: Report of the AAPM Therapy Physics Committee Task Group 180. *Med Phys* 2018;45(5):e84–e99.
26. Alaei P, Spezi E. Imaging dose from cone beam computed tomography in radiation therapy. *Phys Med* 2015;31(7):647–58.
27. Miften M, Olch A, Mihailidis D, Moran J, Pawlicki T, Molineu A, et al. Tolerance limits and methodologies for IMRT measurement-based verification QA: Rec-

- ommendations of AAPM Task Group No. 218. *Med Phys* 2018;45(4):e53–e83.
28. Ding GX, Yu CW. A study on beams passing through hip prosthesis for pelvic radiation treatment. *Int J Radiat Oncol Biol Phys* 2001;51(4):1167–75
 29. Mahuvava C, Du Plessis FCP. Dosimetry effects caused by unilateral and bilateral hip prostheses: a monte carlo case study in megavoltage photon radiotherapy for computed tomography data without metal artifacts. *J Med Phys* 2018;43(4):236–46.
 30. Kung JH, Reft H, Jackson W, Abdalla I. Intensity-modulated radiotherapy for a prostate patient with a metal prosthesis. *Med Dosim* 2001;26(4):305–8.
 31. To D, Xhaferllari I, Liu M, Liang J, Knill C, Nandalur S, et al. Evaluation of VMAT planning strategies for prostate patients with bilateral hip prosthesis. *Technol Cancer Res Treat* 2021;20:15330338211038490.
 32. Soda R, Hatanaka S, Hariu M, Shimbo M, Yamano T, Nishimura K, et al. Evaluation of geometrical uncertainties on localized prostate radiotherapy of patients with bilateral metallic hip prostheses using 3D-CRT, IMRT and VMAT: A planning study. *J Xray Sci Technol* 2020;28(2):243–54.
 33. Gallo JJ, Kaufman I, Powell R, Pandya S, Somnay A, Bossenberger T, et al. Single-fraction spine SBRT end-to-end testing on TomoTherapy, Vero, TrueBeam, and CyberKnife treatment platforms using a novel anthropomorphic phantom. *J Appl Clin Med Phys* 2015;16(1):5120.
 34. Le Fèvre C, Brinkert D, Menoux I, Kuntz F, Antoni D, El Bitar Z, et al. Effects of a metallic implant on radiotherapy planning treatment-experience on a human cadaver. *Chin Clin Oncol* 2020;9(2):14.
 35. Giantsoudi D, De Man B, Verburg J, Trofimov A, Jin Y, Wang G, et al. Metal artifacts in computed tomography for radiation therapy planning: dosimetric effects and impact of metal artifact reduction. *Phys Med Biol* 2017;62(8):R49–R80.